scientific reports

Check for updates

OPEN

Entanglement swapping through the amplitude damping noise channel

Jianbo Xing[1]✉ & Fan Zhang[2,3,4]✉

This paper investigates the degradation mechanism of the photon-number-encoded entanglement swapping protocol under the amplitude damping noise channel. By establishing a beam splitter physical model to simulate the energy dissipation process, the evolution density matrix of the input states $|\psi\rangle_{AB} = \alpha|00\rangle + \beta|11\rangle$ and $|\psi\rangle_{CD} = m|00\rangle + n|11\rangle$ under independent noise channels is analytically derived, and the density matrix, fidelity, and concurrence of the target particle pair after entanglement swapping are presented. Furthermore, for the case where the initial states are maximally entangled states, this paper numerically simulates the variation curves of the fidelity and concurrence of the system after entanglement swapping with the noise parameter. The results show that as the noise intensity increases, both the fidelity and concurrence of the target system exhibit a decreasing trend. Simultaneously, due to the presence of noise, even if the input states are maximally entangled, the entanglement of the target system after swapping may be destroyed. Based on this, the study further deduces the constraint conditions required to maintain system entanglement in this scenario. Given the restrictive effect of these constraints on entanglement maintenance, this paper also specifically examines the fidelity and concurrence of the target state output from entanglement swapping in the case of 50 : 50 beam splitters when the input states are both maximally entangled. The research finds that in this case, since the constraints are not satisfied, even if the input states are maximally entangled, the entanglement of the output state completely disappears.

Keywords Entanglement swapping, Lossy channels

Recently, the concept of quantum entanglement[1]has garnered widespread attention for its central role in quantum cryptography[2], quantum teleportation[3], quantum dense coding[4], quantum metrology[5], quantum telecloning[6], and other domains. To date, a variety of platforms,including trapped ions[7], atomic ensembles[8], photon pairs[9], and superconducting qubits[10], have been utilized to generate entangled states. Beyond these approaches, interactions between atoms and cavity fields have also proven to be an effective mechanism for entanglement generation[11]. Such interactions are typically modeled by the Jaynes-Cummings model (JCM)[12], which, under the rotating wave approximation, describes the coupling between a two-level atom and a single-mode quantized field. Conventionally, it is believed that entanglement generation between particles requires direct interaction. However, entanglement swapping[13] provides a method that circumvents this requirement. This mechanism employs two (or more) pre-entangled quantum subsystems as mediators to generate entanglement between spatially separated particles without direct interaction. Initially proposed for swapping entanglement between particle pairs, the concept was later extended to multipartite systems[14]. Studies have shown that entanglement swapping is also applicable to continuous-variable systems[15], and its unconditional experimental realization has been reported in Ref[16].. Protocols for optimizing entanglement purification via entanglement swapping are presented in Ref[17].. Moreover, entanglement swapping between subsystems in two independent Jaynes–Cummings models is analyzed in Ref[18].. Today, entanglement swapping has become a cornerstone of quantum information science, underpinning key applications such as quantum repeaters, quantum networks, and distributed quantum computing[19–25]. However, real-world quantum systems are open quantum systems[26] and inevitably interact with their environment, leading to decoherence[27]. The phenomenon of decoherence poses a threat to meticulously prepared and preserved entangled states, ultimately undoing their quantum coherence or resulting in a complete reduction to classical states. Therefore, a thorough understanding of how environmental

[1]School of Physics and Astronomy, Beijing Normal University, Beijing 100875, China. [2]Institute for Frontiers in Astronomy and Astrophysics, Beijing Normal University, Beijing 102206, China. [3]Gravitational Wave and Cosmology Laboratory, School of Physics and Astronomy, Beijing Normal University, Beijing 100875, China. [4]Advanced Institute of Natural Sciences, Beijing Normal University at Zhuhai, Zhuhai 519087, China. ✉email: 202321160019@mail.bnu.edu.cn; fnzhang@bnu.edu.cn

noise—particularly when modeled via noise channels—affects the evolution of quantum states, and specifically its impact on key performance metrics in entanglement swapping (such as fidelity and concurrence), is essential for improving the robustness and longevity of entanglement in noisy settings. This constitutes the central focus of the present study. This work aims to analyze specifically the influence of a typical environmental noise—amplitude damping nosie—on the entanglement swapping process. We examine the evolution of entangled states encoded in photon-number-states when subjected to an amplitude damping channel, which models energy dissipation or particle loss. The primary objective is to quantitatively characterize, through rigorous theoretical modeling and calculation, how amplitude damping noise acts on photon-number-encoded entanglement, and to analyze the resulting degradation in key output measures—such as the fidelity and concurrence of the final entangled state—over the course of the swapping protocol. This investigation into the relationship between noise and the evolution of quantum properties (e.g., entanglement) during swapping provides a theoretical basis for optimizing entanglement swapping protocols and enhancing their robustness under amplitude damping.

The structure of this paper is as follows: In "Entanglement Swapping", we briefly review the basic concepts and principles of entanglement swapping. In "Entanglement Swapping via the Amplitude Damping Noise Channel", we focus on the effect of the amplitude damping channel on entanglement swapping for photon-number-encoded entangled states, and present the post-swapping density matrix after the action of the amplitude damping channel. In Section "Results and Discussion", we analyze the fidelity and concurrence of the system after swapping. Numerical simulations are performed for the case of maximally entangled states, showing the fidelity and concurrence of the target system AC, and based on these, the conditions for preserving entanglement in the target system are proposed. In "Conclusion", we give a brief conclusion.

Entanglement swapping

Assume that Alice holds an entangled particle pair *AB*, and Bob holds another entangled particle pair *CD*. Both pairs are initially prepared in the maximally entangled Bell state

$$|\phi^+\rangle = \frac{1}{\sqrt{2}}(|00\rangle + |11\rangle), \tag{1}$$

According to quantum mechanics principles, the total state of the four-particle composite system is given by

$$|\psi\rangle_{ABCD} = |\phi^+\rangle_{AB} \otimes |\phi^+\rangle_{CD}, \tag{2}$$

The state $|\psi\rangle_{ABCD}$ can be re-expressed in terms of the four Bell states for particle pair *AC* and *BD* as follows

$$|\psi\rangle_{ABCD} = \frac{1}{2}(|\phi^+\rangle_{AC}|\phi^+\rangle_{BD} + |\phi^-\rangle_{AC}|\phi^-\rangle_{BD} + |\psi^+\rangle_{AC}|\psi^+\rangle_{BD} + |\psi^-\rangle_{AC}|\psi^-\rangle_{BD}), \tag{3}$$

where $|\phi^-\rangle = \frac{1}{\sqrt{2}}(|00\rangle - |11\rangle)$ and $|\psi^\pm\rangle = \frac{1}{\sqrt{2}}(|01\rangle \pm |10\rangle)$.

To establish entanglement between the spatially separated particles *A* and *C*, Alice and Bob send their respective particles *B* and *D* to a third party, Charlie, via a lossless quantum channel. Upon receiving particles *B* and *D*, Charlie performs a joint Bell-state measurement (BSM) on the composite system *BD*. If the measurement outcome corresponds to the projection onto the Bell state $|\phi^+\rangle$, the post-measurement state of the system, according to the measurement postulate of quantum mechanics, is given by

$$|\psi'\rangle = \frac{\Pi_{\phi^+}|\psi\rangle_{ABCD}}{tr\left(\Pi_{\phi^+}\rho_{ABCD}\right)} = |\phi^+\rangle_{AC}|\phi^+\rangle_{BD}. \tag{4}$$

where $\Pi_{\phi^+} = I_{AC} \otimes |\phi^+\rangle_{BD}\langle\phi^+|_{BD}$. This result demonstrates that although particles *A* and *C* remain spatially separated and have never interacted directly, after performing the Bell state measurement on particles *B* and *D*, they collapse into one of the Bell entangled states. This procedure is known as entanglement swapping.

Entanglement swapping via the amplitude damping noise channel

Assume that Alice and Bob prepare the following photon-number-encoded entangled states, respectively

$$\begin{aligned} |\psi\rangle_{AB} &= \alpha|00\rangle + \beta|11\rangle, \\ |\psi\rangle_{CD} &= m|00\rangle + n|11\rangle. \end{aligned} \tag{5}$$

where $|\alpha|^2 + |\beta|^2 = |m|^2 + |n|^2 = 1$. Alice and Bob then send particles *B* and *D* to the third party, Charlie, via amplitude damping channels. For photon-number-encoded entangled states, the amplitude damping channel can be modeled by a beam splitter. The unitary transformation Hamiltonian of the beam splitter can be written as[28]

$$B = \exp\left[\theta\left(a^\dagger b - a b^\dagger\right)\right]. \tag{6}$$

where a ($a^\dagger$) and b ($b^\dagger$) are both bosonic annihilation (creation) operators.

Suppose the input state is $|\psi\rangle_{AB} = \alpha|00\rangle + \beta|11\rangle$ and the environment is initially in the vacuum state, then the output state after the beam splitter action is

$$
\begin{aligned}
|\tilde{\psi}\rangle &= I_A \otimes B|\psi\rangle_{AB} \otimes |0\rangle_E \\
&= I_A B(\alpha|000\rangle + \beta|110\rangle) \\
&= \alpha|000\rangle + \beta\cos\theta|110\rangle - \beta\sin\theta|101\rangle,
\end{aligned} \tag{7}
$$

Tracing out the environmental degree of freedom yields the density matrix for system AB

$$
\rho_{AB} = \begin{pmatrix} |\alpha|^2 & 0 & 0 & \alpha\beta^*\cos\theta_1 \\ 0 & 0 & 0 & 0 \\ 0 & 0 & |\beta|^2\sin^2\theta_1 & 0 \\ \alpha^*\beta\cos\theta_1 & 0 & 0 & |\beta|^2\cos^2\theta_1 \end{pmatrix}, \tag{8}
$$

The evolution of the composite system AB, under the local amplitude damping channel on qubit B, is equivalently described by the Kraus operators $\{E_k\}$ acting on the two-qubit space: $E_0 = I_A \otimes E_0^{(B)}$ and $E_1 = I_A \otimes E_1^{(B)}$, where $E_0^{(B)} = |0\rangle\langle 0| + \cos\theta_1|1\rangle\langle 1|$ and $E_1^{(B)} = \sin\theta_1|0\rangle\langle 1|$ are the single-qubit Kraus operators for the channel. Setting the damping probability $p = \sin^2\theta_1$, these correspond to the standard form $E_0^{(B)} = \begin{pmatrix} 1 & 0 \\ 0 & \sqrt{1-p} \end{pmatrix}$ and $E_1^{(B)} = \begin{pmatrix} 0 & \sqrt{p} \\ 0 & 0 \end{pmatrix}$ used in the operator-sum representation of the amplitude damping channel[29]. And the density matrix in Eq. (8) is obtained via $\rho_{AB} = \sum_{k=0}^{1} E_k \rho_{in} E_k^\dagger$.

Similarly, the density matrix of system DC is given by

$$
\rho_{DC} = \begin{pmatrix} |m|^2 & 0 & 0 & mn^*\cos\theta_2 \\ 0 & |n|^2\sin^2\theta_2 & 0 & 0 \\ 0 & 0 & 0 & 0 \\ m^*n\cos\theta_2 & 0 & 0 & |n|^2\cos^2\theta_2 \end{pmatrix}. \tag{9}
$$

After receiveing particles B and D, Charlie performs a joint Bell-state measurement on the BD systems, described by the projector $I_A \otimes |\phi^+\rangle_{BD}\langle\phi^+|_{BD} \otimes I_C$. Taking the partial trace over BD, the density matrix of system AC is

$$
\rho_{AC} = \begin{bmatrix} -\frac{|\alpha|^2|m|^2}{\sigma_4} & 0 & 0 & \frac{\alpha m\beta^* n^*\cos\theta_1\cos\theta_2}{\sigma_1} \\ 0 & \frac{|\alpha|^2\sin^2\theta_2\sigma_2}{\sigma_4} & 0 & 0 \\ 0 & 0 & \frac{|m|^2\sin^2\theta_1\sigma_3}{\sigma_4} & 0 \\ \frac{\beta n\alpha^* m^*\cos\theta_1\cos\theta_2}{\sigma_1} & 0 & 0 & \frac{\sigma_3\sigma_2(-2\sin^2\theta_1\sin^2\theta_2+\sin^2\theta_1+\sin^2\theta_2-1)}{\sigma_4} \end{bmatrix}, \tag{10}
$$

where the parameters are given by

$$
\sigma_1 = 2\cos^2\theta_1\cos^2\theta_2(|\alpha|^2-1)(|m|^2-1) + \cos^2\theta_1(|\alpha|^2-1) + \cos^2\theta_2(|m|^2-1) + 1, \tag{11}
$$

$$
\sigma_2 = |m|^2 - 1, \tag{12}
$$

$$
\sigma_3 = |\alpha|^2 - 1, \tag{13}
$$

$$
\sigma_4 = -2(|\alpha|^2-1)(|m|^2-1)\cos^2\theta_1\cos^2\theta_2 - (|\alpha|^2-1)\cos^2\theta_1 - (|m|^2-1)\cos^2\theta_2 - 1 = -\sigma_1. \tag{14}
$$

Results and discussion

The derivation of the post-swapping density matrix for system AC within the amplitude damping channel, as presented above, now enables us to thoroughly assess the degradation of quantum resources. For this purpose, we employ two critical metrics: fidelity, to evaluate state quality, and concurrence, to measure the degree of entanglement.

Fidelity

As a cornerstone of quantum information science, quantum state fidelity provides a crucial measure of the closeness between two quantum states, ranging from 0 (completely distinguishable) to 1 (identical). It is indispensable for evaluating the accuracy of quantum protocols, especially under decoherence. In this work, fidelity specifically serves to benchmark the effect of the amplitude damping channel on our entanglement swapping protocol, by quantifying the discrepancy between the ideal Bell state and the actual output state. For a target pure state $|\psi(0)\rangle$, the fidelity of the output state $\rho_s(t)$ is defined as[30]

$$
F = \langle\psi(0)|\rho_s|\psi(0)\rangle, \tag{15}
$$

Therefore, compared to the Bell state $|\phi^+\rangle$, the fidelity of system AC is $F = \frac{B}{A}$, where

$$
\begin{aligned}
A = {} & |\alpha|^2|m|^2 + (|\alpha|^2-1)(|m|^2-1)(\sin^2\theta_1\sin^2\theta_2 + \cos^2\theta_1\cos^2\theta_2) \\
& + \frac{\alpha m\cos\theta_1\cos\theta_2(|\alpha|^2-1)(|m|^2-1)}{\beta n} + \frac{\beta n|\alpha|^2|m|^2\cos\theta_1\cos\theta_2}{\alpha m}.
\end{aligned} \tag{16}
$$

$$B = 4(|\alpha|^2 - 1)(|m|^2 - 1)\cos^2\theta_1\cos^2\theta_2 + 2(|\alpha|^2 - 1)\cos^2\theta_1 + 2(|m|^2 - 1)\cos^2\theta_2 + 2. \tag{17}$$

Concurrence

Measuring the degree of entanglement of an entangled state is a core issue in quantum information theory. There are several important measures, such as entanglement entropy, entanglement of formation[31], concurrence[32], and negativity[33]. Here we use concurrence to measure the entanglement degree of system *AB*. The concurrence for a two-qubit system is given by

$$C(\rho) = \max\left(0, \sqrt{\lambda_1} - \sqrt{\lambda_2} - \sqrt{\lambda_3} - \sqrt{\lambda_4}\right), \tag{18}$$

where λ_is are the eigenvalues of the matrix *R*, arranged in descending order ($\lambda_1 \geq \lambda_2 \geq \lambda_3 \geq \lambda_4$), and *R* satisfies

$$R = \sqrt{\sqrt{\rho}\sqrt{\tilde{\rho}}\sqrt{\rho}}, \tag{19}$$

Here, $\tilde{\rho}$ is the spin-flipped state of ρ

$$\tilde{\rho} = (\sigma_y \otimes \sigma_y)\rho^*(\sigma_y \otimes \sigma_y), \tag{20}$$

where $\sigma_y = \begin{pmatrix} 0 & -i \\ i & 0 \end{pmatrix}$.

For an X-shaped density matrix, the following formula

$$C(\rho) = 2\max\left(0, |\rho_{14}| - \sqrt{\rho_{22}\rho_{33}}, |\rho_{23}| - \sqrt{\rho_{11}\rho_{44}}\right), \tag{21}$$

can be used to calculate its concurrence. Therefore, the concurrence of state ρ_{AC} is

$$C(\rho) = 2 \cdot \max\left\{0, |\rho_{14}| - \sqrt{\rho_{22}\rho_{33}}\right\}. \tag{22}$$

where negative terms have been omitted.

Numerical simulation

To further quantitatively analyze the destructive mechanism of the noise channel on entanglement swapping, this section conducts numerical simulations for maximally entangled initial states. The concurrence and fidelity are directly calculated from the density matrix, and the graphs showing the relationship between these two quantities and the amplitude damping noise strength parameter θ are presented to quantitatively characterize the degradation law of quantum resources.

For the case where the initial state is a maximally entangled state, the fidelity of system *AC* after entanglement swapping is

$$F = \frac{(1 + \cos\theta_1\cos\theta_2)^2 + \sin^2\theta_1\sin^2\theta_2}{4(1 + \sin^2\theta_1\sin^2\theta_2)}, \tag{23}$$

And the concurrence (Note that the complete concurrence should be Eq. (22), but for convenience, we will only examine the behavior of $2\left\{|\rho_{14}| - \sqrt{\rho_{22}\rho_{33}}\right\}$ here) is

$$C_\rho = \frac{\cos\theta_1\cos\theta_2 - \sqrt{1 - \cos^2\theta_1}\sqrt{1 - \cos^2\theta_2}}{2 + \cos^2\theta_1\cos^2\theta_2 - \cos^2\theta_1 - \cos^2\theta_2}. \tag{24}$$

For photon-number-encoded entangled states, the amplitude damping noise is simulated by a beam splitter. Therefore, the parameters $\cos\theta$ and $\sin\theta$ are actually the transmissivity *t* and reflectivity *r* of the beam splitter, respectively, satisfying $t^2 + r^2 = 1$. For simplified expression, *t* and *r* will be used in the following discussion. It should be noted that t_1 and r_1 correspond to the transmissivity and reflectivity of the beam splitter acting on qubit *B*, while t_2 and r_2 correspond to those acting on qubit *D*.

Figure 1 illustrates the variation of the swapped entanglement fidelity *F* for system *AC* with the beam splitter transmissivity *t*, under the condition that both initial states are maximally entangled. Figure 2 simulates the relationship between the fidelity *F* and the transmissivity t_2 for three specific cases: when $t_1 = \frac{1}{2}$, when $t_1 = \frac{\sqrt{2}}{2}$, $t_1 = \frac{\sqrt{3}}{2}$ and when $t_1 = t_2$. Figure 3 simulates the relationship between the fidelity *F* and the reflectivity r_2 for three specific cases: when $r_1 = \frac{\sqrt{3}}{2}$, when $r_1 = \frac{\sqrt{2}}{2}$, $r_1 = \frac{1}{2}$ and when $r_1 = r_2$.

The results demonstrate that for maximally entangled initial states, the fidelity *F* of the composite system *AC* after entanglement swapping increases with the transmissivity *t* of the beam splitter. Consequently, it decreases as the reflectivity *r* rises. This occurs because the square of the reflectivity, $r^2 = \sin^2\theta = p$, directly represents the photon loss probability[28]. As *r* increases, this loss probability rises, thereby reducing the chance of successful photon transmission through the channel. This leads to the observed decrease in overall fidelity.

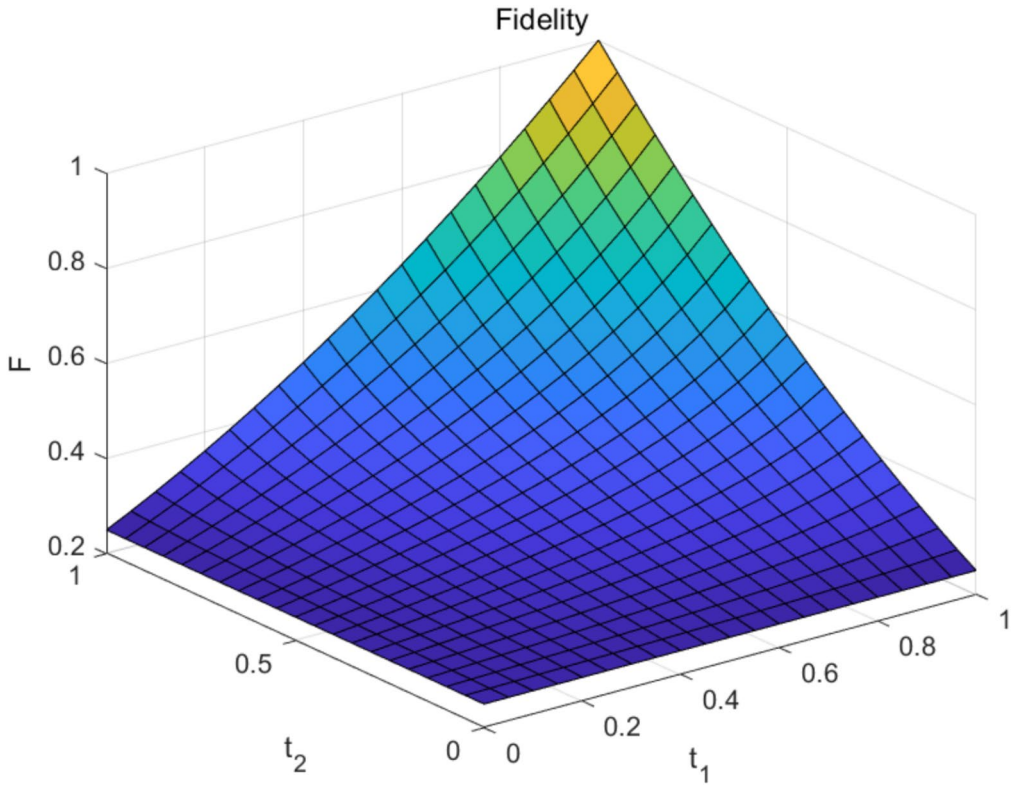

Fig. 1. Fidelity F versus transmissivity t_1.

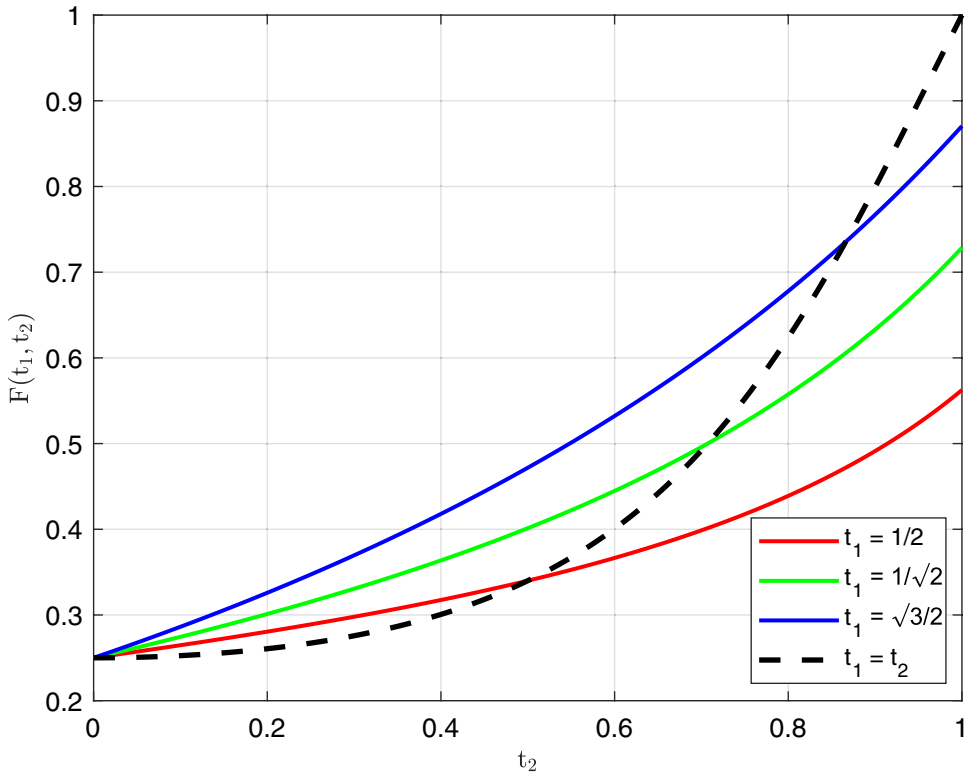

Fig. 2. The relationship between fidelity F and t_2 when t_1 takes different values.

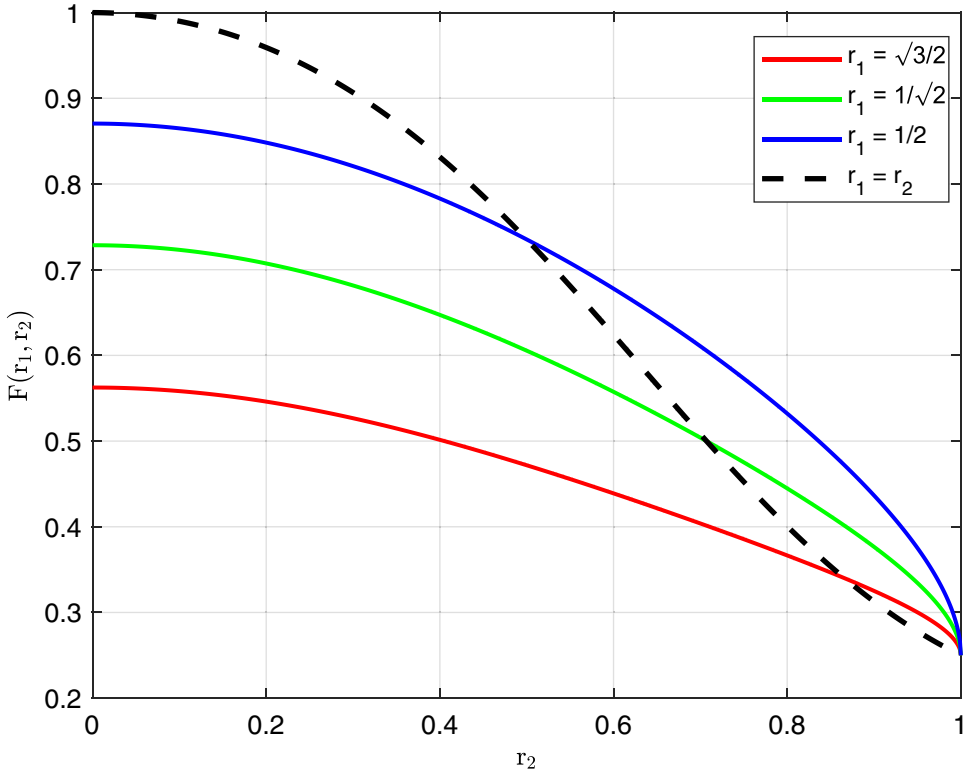

Fig. 3. Fidelity F versus reflectivity r_1 and r_2.

Figure 4 shows the relationship between the concurrence C of system AC after entanglement swapping and the beam splitter transmissivity t for the case where the initial states are maximally entangled. Figure 5 simulates the relationship between concurrence C and t for cases where t_1 equals to $\frac{1}{2}, \frac{\sqrt{2}}{2}, \frac{\sqrt{3}}{2}$ and $t_1 = t_2$, respectively. Figure 6 simulates the relationship between concurrence C and r for cases where r_1 equals to $\frac{\sqrt{3}}{2}, \frac{\sqrt{2}}{2}, \frac{1}{2}$ and $r_1 = r_2$, respectively.

A similar pattern is observed for the concurrence: as t increases—corresponding to a weakening of the amplitude damping noise or channel loss—the concurrence of system AC also exhibits an overall upward trend. However, Fig. 5 reveals that the presence of entanglement in system AC (i.e., $C > 0$) is not automatically ensured by the swapping process itself. This is due to the destructive effect of the noise channel, which under certain parameter conditions can destroy entanglement after swapping.

To quantify when entanglement is preserved, we derive the constraint conditions from the analytical expression for concurrence (e.g., Eq. (24). Specifically, since the denominator of Eq. (24) is always positive, the condition for entanglement existence ($C > 0$) simplifies to the requirement that the numerator must be positive. This yields the practical and concise criterion that the reflection and transmission coefficients must satisfy $t_1 t_2 > r_1 r_2$.

This constraint has immediate practical implications. Consider the case of 50 : 50 beam splitters. Here, $r_1 r_2 = t_1 t_2 = \frac{1}{2}$, which directly violates the condition $t_1 t_2 > r_1 r_2$. As a result, the concurrence drops to zero ($C = 0$), indicating a complete loss of entanglement. Consequently, for any given channel loss (reflectivity), this criterion serves as an immediate and definitive predictor for whether entanglement will survive the swapping process or be completely destroyed.

Furthermore, several points regarding fidelity and concurrence in the figures require clarification.

Firstly, since entanglement between A and C is established via entanglement swapping, it is necessary that entanglement between A and B (C and D) persists after passing through the damping channels. According to Eq. (8) and and the Peres-Horodecki positive partial transpose (PPT) criterion[34], the condition for entanglement between A and B is

$$\cos\theta_1 = t_1 \neq 0 \quad \text{and} \quad \alpha\beta \neq 0, \tag{25}$$

which corresponds to incomplete damping. Since t represents transmissivity and satisfies $0 < t < 1$, the condition for AB entanglement is effectively

$$0 < t_1 < 1 \quad \text{and} \quad \alpha\beta \neq 0. \tag{26}$$

Similar conditions can also be derived for system CD.

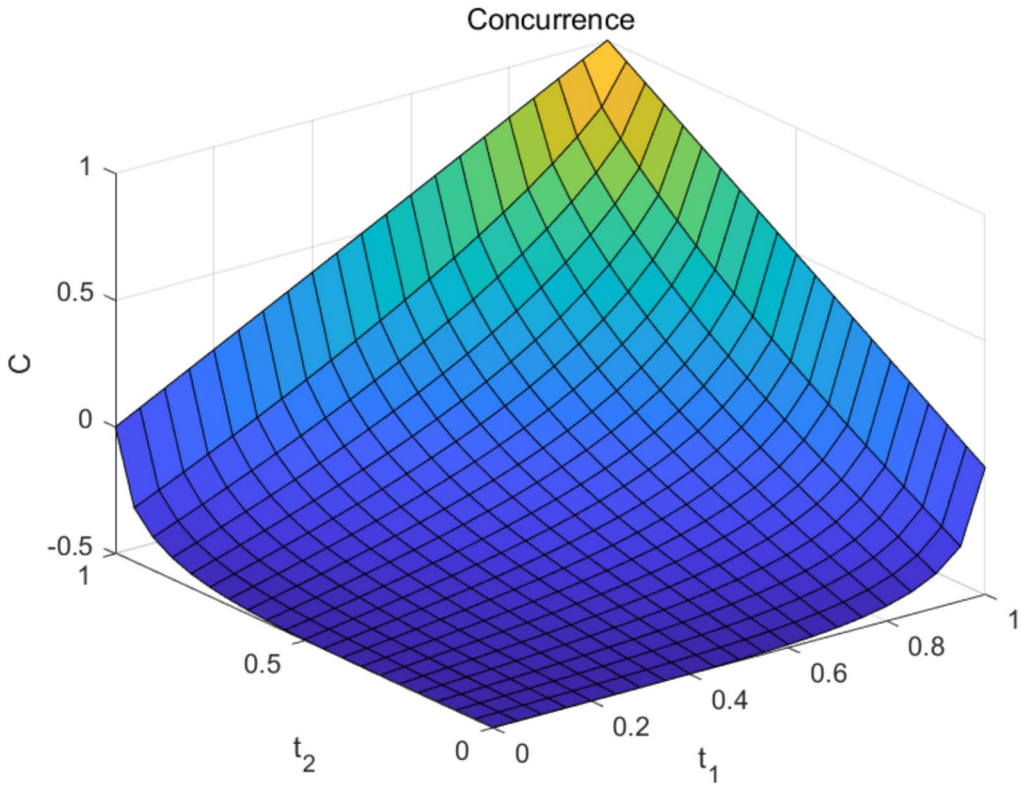

Fig. 4. Concurrence C versus transmissivity t_1 and t_2.

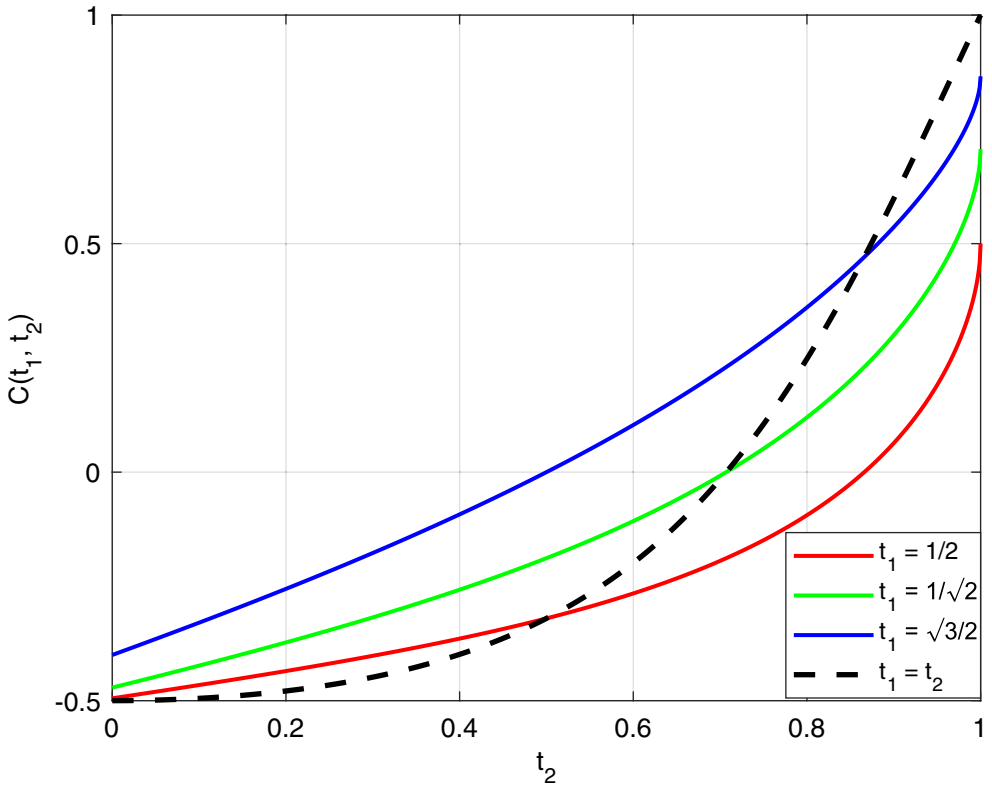

Fig. 5. The relationship between Concurrence C and r_2 when r_1 takes different values.

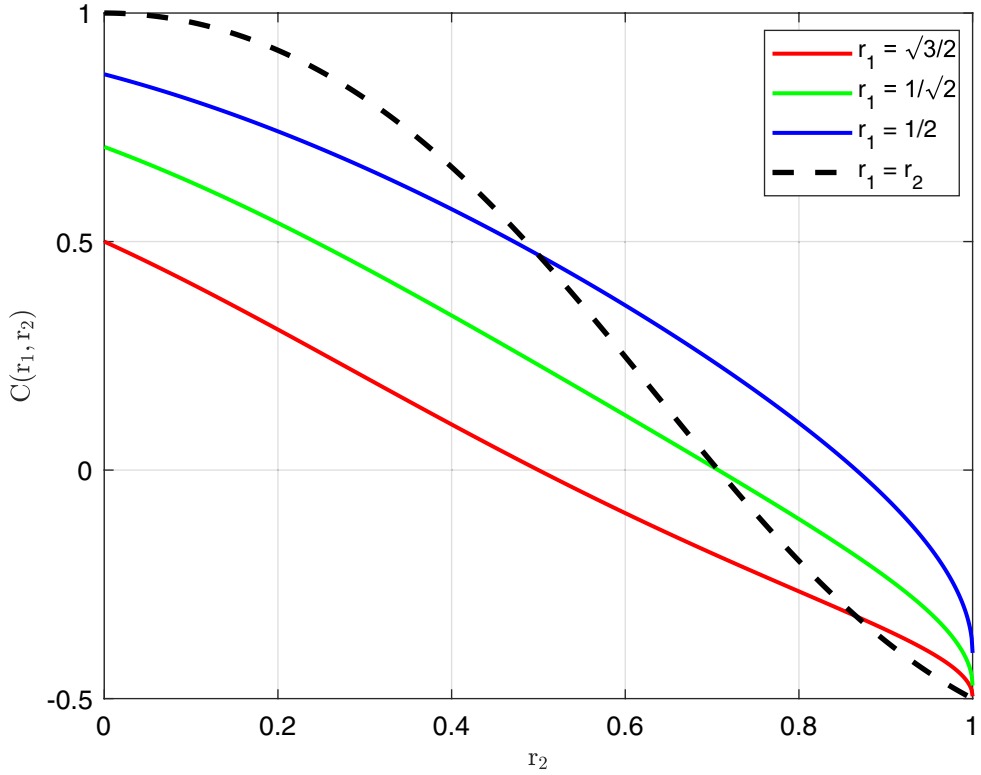

Fig. 6. Fidelity F versus reflectivity r_1 and r_2.

Although complete damping ($t = 0$) is physically unattainable, our derivation, viewed mathematically, naturally encompasses both the completely damped case ($t = 0$) and the ideal noiseless case ($t = 1$).

We now examine the two extreme cases: $t = 0$ and $t = 1$.

When one of the channels is completely damped (e.g., $t_2 = 0$), Fig. 5 shows that the concurrence between A and C is zero. (Note that the complete concurrence is $C(\rho) = 2 \cdot \max\left\{0, |\rho_{14}| - \sqrt{\rho_{22}\rho_{33}}\right\}$, where $2(|\rho_{14}| - \sqrt{\rho_{22}\rho_{33}})$ is Eq. (24)). Consequently, no entanglement can be established between A and C via swapping. This result is expected: from Eq. (9), when $t_2 = 0$, system CD decays into a separable mixed state after passing through the channel, namely

$$\rho_{DC} = |0_D\rangle\langle 0_D| \otimes \frac{I_C}{2}. \tag{27}$$

where I_C is the Identity operator. So we cannot establish entanglement between AC via entanglement swapping. Meanwhile, it is worth noting that when one of the channels is fully damped, the fidelity of the AC pair is always 1/4, regardless of the parameters of the other channel. This occurs because the complete damping forces the state of AC into the product form $\rho_{AC} = \rho_A \otimes \frac{I_c}{2}$. In this state, the specific off-diagonal elements between $|00\rangle$ and $|11\rangle$ vanish. Consequently, the overlap (fidelity) with $|\phi^+\rangle$ depends only on the classical diagonal probabilities of ρ_A, whose sum is always unity. This results in a constant fidelity of 1/4, independent of the parameter θ_1 that characterizes the initial entangled state of AB.

When both channels are lossless channels ($t_1 = t_2 = 1$), the state of AC after entanglement swapping must be a Bell state, and its concurrence must also be one. This is confirmed by the black dashed line in Fig. 5.

Finally, our results show that for $t_2 = 0$ the concurrence of AC is zero while the fidelity remains positive. This is not contradictory:fidelity measures the similarity between two states but cannot serve as a criterion for entanglement. A clear example is the separable $\rho_{AB} = \frac{I_A}{2} \otimes \frac{I_B}{2}$ (with I_A and I_B are both 2×2 Identity matrix), whose fidelity is 1/4 compared to $|\phi^+\rangle$ even though AB is unentangled.

Conclusion

This study quantitatively characterizes the impact of amplitude damping noise on the entanglement swapping protocol, analytically deriving the density matrix and fidelity of the output state. The key finding reveals that even when the input states are maximally entangled, the destructive effect of the noise channel can still cause the output state after entanglement swapping to lose its entanglement. Based on this, the paper further provides the constraint conditions required to maintain output state entanglement in the case of maximally entangled input states. For 50 : 50 beam splitters, although the input states are maximally entangled, the constraint condition is not satisfied, resulting in complete disappearance of entanglement in the output state ($C = 0$). This

result underscores the urgency of noise suppression in practical quantum networks and provides a theoretical benchmark for optimizing the design of quantum repeaters.

Data availability

The datasets generated during the current study are available from the corresponding author on reasonable request.

Received: 1 October 2025; Accepted: 3 February 2026
Published online: 09 February 2026

References

1. Horodecki, R., Horodecki, P., Horodecki, M. & Horodecki, K. Quantum entanglement. *Rev. Mod. Phys.* **81**, 865–942. https://doi.org/10.1103/RevModPhys.81.865 (2009).
2. Ekert, A. K. Quantum cryptography based on bell's theorem. *Phys. Rev. Lett.* **67**, 661–663. https://doi.org/10.1103/PhysRevLett.67.661 (1991).
3. Braunstein, S. L. & Mann, A. Measurement of the bell operator and quantum teleportation. *Phys. Rev. A* **51**, R1727–R1730. https://doi.org/10.1103/PhysRevA.51.R1727 (1995).
4. Mattle, K., Weinfurter, H., Kwiat, P. G. & Zeilinger, A. Dense coding in experimental quantum communication. *Phys. Rev. Lett.* **76**, 4656–4659. https://doi.org/10.1103/PhysRevLett.76.4656 (1996).
5. Richter, T. & Vogel, W. Nonclassical characteristic functions for highly sensitive measurements. *Phys. Rev. A* **76**, 053835. https://doi.org/10.1103/PhysRevA.76.053835 (2007).
6. Murao, M., Jonathan, D., Plenio, M. B. & Vedral, V. Quantum telecloning and multiparticle entanglement. *Phys. Rev. A* **59**, 156–161. https://doi.org/10.1103/PhysRevA.59.156 (1999).
7. Turchette, Q. A. et al. Deterministic entanglement of two trapped ions. *Phys. Rev. Lett.* **81**, 3631–3634. https://doi.org/10.1103/PhysRevLett.81.3631 (1998).
8. Julsgaard, B., Kozhekin, A. & Polzik, E. S. Experimental long-lived entanglement of two macroscopic objects. *Nature* **413**, 400–403. https://doi.org/10.1038/35096524 (2001).
9. Aspect, A., Grangier, P. & Roger, G. Experimental tests of realistic local theories via bell's theorem. *Phys. Rev. Lett.* **47**, 460–463. https://doi.org/10.1103/PhysRevLett.47.460 (1981).
10. Izmalkov, A. et al. Evidence for entangled states of two coupled flux qubits. *Phys. Rev. Lett.* **93**, 037003. https://doi.org/10.1103/PhysRevLett.93.037003 (2004).
11. Baghshahi, H. R., Tavassoly, M. K. & Faghihi, M. J. Entanglement analysis of a two-atom nonlinear jaynes–cummings model with nondegenerate two-photon transition, kerr nonlinearity, and two-mode stark shift. *Laser Physics* **24**, 125203. https://doi.org/10.1088/1054-660X/24/12/125203 (2014).
12. Jaynes, E. & Cummings, F. Comparison of quantum and semiclassical radiation theories with application to the beam maser. *Proceedings of the IEEE* **51**, 89–109. https://doi.org/10.1109/PROC.1963.1664 (1963).
13. Żukowski, M., Zeilinger, A., Horne, M. A. & Ekert, A. K. event-ready-detectors bell experiment via entanglement swapping. *Phys. Rev. Lett.* **71**, 4287–4290. https://doi.org/10.1103/PhysRevLett.71.4287 (1993).
14. Bose, S., Vedral, V. & Knight, P. L. Multiparticle generalization of entanglement swapping. *Phys. Rev. A* **57**, 822–829. https://doi.org/10.1103/PhysRevA.57.822 (1998).
15. Polkinghorne, R. E. S. & Ralph, T. C. Continuous variable entanglement swapping. *Phys. Rev. Lett.* **83**, 2095–2099. https://doi.org/10.1103/PhysRevLett.83.2095 (1999).
16. Jia, X. et al. Experimental demonstration of unconditional entanglement swapping for continuous variables. *Phys. Rev. Lett.* **93**, 250503. https://doi.org/10.1103/PhysRevLett.93.250503 (2004).
17. Shi, B.-S., Jiang, Y.-K. & Guo, G.-C. Optimal entanglement purification via entanglement swapping. *Phys. Rev. A* **62**, 054301. https://doi.org/10.1103/PhysRevA.62.054301 (2000).
18. Liao, Q. H., Fang, G. Y., Wang, Y. Y., Ahmad, M. A. & Liu, S. Entanglement swapping in two independent jaynes-cummings models. *The European Physical Journal D* **61**, 475–479. https://doi.org/10.1140/epjd/e2010-00261-x (2011).
19. Jiang, L. et al. Quantum repeater with encoding. *Phys. Rev. A* **79**, 032325. https://doi.org/10.1103/PhysRevA.79.032325 (2009).
20. Hensen, B. et al. Loophole-free bell inequality violation using electron spins separated by 1.3 kilometres. Nature **526**, 682–686, 10.1038/nature15759 (2015).
21. Gyongyosi, L. & Imre, S. Scalable distributed gate-model quantum computers. *Scientific Reports* **11**, 5172. https://doi.org/10.1038/s41598-020-76728-5 (2021).
22. Hong, S. et al. Quantum enhanced multiple-phase estimation with multi-mode n00n states. *Nature Communications* **12**, 5211. https://doi.org/10.1038/s41467-021-25451-4 (2021).
23. Pompili, M. et al. Realization of a multinode quantum network of remote solid-state qubits. *Science* **372**, 259–264. https://doi.org/10.1126/science.abg1919 (2021).
24. Azuma, K. et al. Quantum repeaters: From quantum networks to the quantum internet. *Rev. Mod. Phys.* **95**, 045006. https://doi.org/10.1103/RevModPhys.95.045006 (2023).
25. Kim, D.-H. et al. Distributed quantum sensing of multiple phases with fewer photons. *Nature Communications* **15**, 266. https://doi.org/10.1038/s41467-023-44204-z (2024).
26. Breuer, H.-P. & Petruccione, F. The theory of open quantum systems (OUP Oxford, 2002).
27. Zurek, W. H. Decoherence, einselection, and the quantum origins of the classical. *Rev. Mod. Phys.* **75**, 715–775. https://doi.org/10.1103/RevModPhys.75.715 (2003).
28. Nielsen, M. A. & Chuang, I. L. Quantum computation and quantum information (Cambridge university press, 2010).
29. Hu, M.-L. & Fan, H. Evolution equation for geometric quantum correlation measures. *Phys. Rev. A* **91**, 052311. https://doi.org/10.1103/PhysRevA.91.052311 (2015).
30. Jozsa, R. Fidelity for mixed quantum states. *Journal of Modern Optics* **41**, 2315–2323. https://doi.org/10.1080/09500349414552171 (1994).
31. Wootters, W. K. Entanglement of formation of an arbitrary state of two qubits. *Phys. Rev. Lett.* **80**, 2245–2248. https://doi.org/10.1103/PhysRevLett.80.2245 (1998).
32. Hill, S. A. & Wootters, W. K. Entanglement of a pair of quantum bits. *Phys. Rev. Lett.* **78**, 5022–5025. https://doi.org/10.1103/PhysRevLett.78.5022 (1997).
33. Życzkowski, K., Horodecki, P., Sanpera, A. & Lewenstein, M. Volume of the set of separable states. *Phys. Rev. A* **58**, 883–892. https://doi.org/10.1103/PhysRevA.58.883 (1998).
34. Peres, A. Separability criterion for density matrices. *Phys. Rev. Lett.* **77**, 1413–1415. https://doi.org/10.1103/PhysRevLett.77.1413 (1996).

Acknowledgements
F. Zhang thanks Jianbo Xing for helpful discussions.

Author contributions
J.B. X. wrote the main text, prepared all figures and conducted the analysis. F.Z. reviewed the manuscript. F.Z. supervised the whole process.

Funding
This work is supported by the National Natural Science Foundation of China grant 12021003, and National Key Research and Development Program of China grant 2023YFC2205801.

Declarations

Competing interests
The authors declare no competing interests.

Additional information
Correspondence and requests for materials should be addressed to J.X. or F.Z.

Reprints and permissions information is available at www.nature.com/reprints.

Publisher's note Springer Nature remains neutral with regard to jurisdictional claims in published maps and institutional affiliations.